International Journal of
INTELLIGENT SYSTEMS AND APPLICATIONS IN ENGINEERING
ISSN:2147-6799 www.ijisae.org Original Research Paper

A Technique Based on Supervised Machine Learning for the Generation of Regulatory Barrier Components in Robotics

[1]Dr. Trapty Agarwal, [2]Sanjeev Kumar Mandal, [3]Vijay Kumar Pandey, [4]Dr. Jaimine Vaishnav, [5]Abhinav Mishra

Submitted: 09/01/2024 **Revised**: 15/02/2024 **Accepted**: 23/02/2024

Abstract: Regulatory barrier components are mathematical compositions to ensure the security of robotic systems. Real-time performance with instantaneous control synthesis requirements may be accomplished for robots by integrating them in quadratic programming as restrictions optimization trouble. The safe zones occasionally need to be approximated online from sensor data, even though prevalent use has assumed a complete understanding of the safety barrier operations. The relevant barrier function in these circumstances has to be created online. The learning approach for predicting control barrier functions from sensor data is described in this research. This allows the system to operate safely in regions of unknown state space. The barrier function definition, in this case, is given by a Deep-AntNeuro ColonyNet (D-ANCN) classifier based on sets of safe and dangerous states gleaned from sensor readings. There are theoretical safety assurances offered. Results from experimental simulations using the Robot Operating System (ROS) to demonstrate the safe operation of a unidirectional robot using LiDAR.

Keywords: *Regulatory Barrier Components, Sensor Data, Deep- Antneuro Colonynet (D-ANCN), Robot Operating System (ROS), Machine learning (ML)*

1. Introduction

Security and regulation requirements of robotic systems are of utmost relevance in the quickly developing field of robotics. Some regulatory constraints must be overcome for robotics applications to ensure their safe operation and societal integration. However, creating regulatory barrier components may be difficult and time-consuming, requiring in-depth knowledge of laws, regulations, and robots [1]. Using supervised ML methods is a viable strategy to tackle this problem. In ML under supervision, a model is trained on a labeled dataset to produce new samples or make predictions based on the patterns and correlations discovered from the data. Automating the creation of regulatory barrier components for robots is now achievable by utilizing the strength of ML algorithms [2]. If regulations are well crafted, they may affect the directions that innovation takes to benefit society. The advantages of developing technology may be valuable despite this possibility, although they are less definite. These are thought to change over time as complementary assets are added and technology develops. As a result, creating a degree of control that is suitable may be exceedingly challenging [3]. Supervised ML algorithms distinguish between legal compliance and non-compliance in robotic systems by identifying significant traits and patterns.

The trained model may then be applied to build regulatory barrier components specifically suited to certain applications or estimate compliance levels for future robotic systems [4]. The designed controller for a high degree of freedom (DOF) upright robotics with a variety of degrees of under actuation (DOUs), regardless of whether the robot is "fully actuated," seek to take into account the limited ability of heel forces to affect the device's overall performance [5]. The robot system, which includes Hand Guiding (HG), Safety-rated Monitored Stop (SMS), Speed and Separation Monitoring (SSM), Power and Force Limiting (PFL), etc. SSM and PFL may be used, in particular, when people and robots work together in a shared workplace. In SSM, the major goal is to prevent any human-robot collisions by keeping an eye on the robot's speed and adjusting it in accordance with the operator's location and, perhaps, speed in the safe area [6]. In particular, the robot must always travel at a pace that will enable it to stop completely before coming into contact with the operator, enabling the operator's distance to be taken into account while determining the safe robot speed. On the other hand, PFL permits physical contact between a robot and an operator while still ensuring the appropriate level of human safety by restricting power and force to

[1]*Maharishi University of Information Technology, Lucknow, India - 226036, Email Id- trapty@muit.in, Orcid Id- 0009-0007-4081-4999*
[2]*Jain (Deemed to be University), Bangalore, Karnataka, India, Email Id- km.sanjeev@jainuniversity.ac.in, Orcid Id- 0000-0002-5562-2486*
[3]*Vivekananda Global University, Jaipur vijay_pandey@vgu.ac.in, Orcid Id- 0000-0002-5258-4779*
[4]*Department of ISME, ATLAS SkillTech University, Mumbai, Maharashtra, India, Email Id- jaimine.vaishnav@atlasuniversity.edu.in, Orcid Id- 0009-0003-9582-3420*
[5]*Chitkara University, Rajpura- 140417, Punjab, India, abhinav.mishra.orp@chitkara.edu.in, https://orcid.org/0009-0005-9856-6727*

levels below which injuries are not anticipated [7].

2. Related Work

The study [8] provided a conceptual framework to assist upcoming researchers in creating and simulating a similar model. Based on a recently developed IoRT control mechanism, they are improved by utilizing algorithms for reinforcement learning and AI. Also known as adaptive Kalman filtering (AKF), the technique is used to track robots and lessen noise in sensors. It is essential to cultivate and model the attitude of mind. A potential method for independently retraining complicated behaviors from scarce sensor input is deep reinforcement learning (RL). The article [9] presented the notable technical advancements in digital agriculture. Big information research and approaches based on AI solve the productivity and sustainability issues in agricultural production. A highly mechanized and data-intensive business, agriculture will be transformed by emerging new applications from old farming practices. The research [10] proposed that many surgical instruments may now function concurrently inside the human body more effectively and at less expense because of advanced sensing, actuation, and automated control technology. Despite advancements, existing surgical intervention systems cannot carry out independent activities and reach cognitive conclusions comparable to those made by humans. The article [11] examined them, reviewing the existing degree of deep learning (DL) and concluding with some of its significant disadvantages for COVID-19 application. Interpretability, Generalisation Metrics, Learning from Restricted Labelled Data, and Data Privacy are some of these limits. Uses of processing of spoken language include information retrieval, query response, mistake identification, public opinion evaluation, and mining COVID-19 research. Medical analysis of images, environmental intelligence, and vision-based robots are all examples of computer vision applications. The study [12] examined how to modify present methodologies and frameworks to allow moral data sharing for ML, security, and legislation prohibiting medical data sharing. A healthcare system based on ML that is free of the sample, annotator, and chronological bias may be constructed using these technologies. These AI-based healthcare imaging systems will fully replace current ones to improve patient care and save costs. Deployed in healthcare institutions across the globe, particularly in rural regions. The study [13] examined the dynamical distal-end pressure predictions of a bendable endoscope robot made using a two-stage data-driven technique in the article without making the supposition. Stage One: Depending on the proximal-end pressure reactions of the machine to a probe message, a convolutional neural network estimates the sheath cumulative bending angle; Stage Two: Innovative estimations of the robot's distal-end pressure are made using a mixture of two extended-short-term recall algorithms that have been already trained people bend at ratios that are most similar to the expected angle.

The article [14] determined that reducing capital expenses, improving network efficiency, and creating new income streams are the main goals of AI/ML integration inside wireless technology. DL AI approaches have replaced conventional computations, significantly reducing energy use and enhancing system performance. Additionally, the use of algorithms for ML enables portable networking service vendors to (i) offer advanced automation levels from sent ML and artificially intelligent structures applicable at the system the edge; (ii) implement based on applications customers steering throughout access point networks; (iii) enable fluid network slicing for addressing scenarios that have the differing quality of service specifications; and (iv) allow ubiquitous connectivity across the various 6G communication systems. The study [15] proposed the first comprehensive assessments of Robotics and Artificial Intelligence (RAI) for the marine renewable power sector is presented in the research. The most recent technology in RAI is examined regarding business and government demand for offshore energy academics in terms of present and potential conditions. A thorough analysis of the funding, rules, and skill-building needed to facilitate RAI adoption is also included in the assessment. The research [16] provided an ML architecture based on Control Lyapunov Functions (CLFs) for generic robots to adjust to unmodeled and parameterized instability behaviors. They suggested technique iteratively updates estimations of the derivatives of the Lyapunov equation and enhances the controller to give a quadratic programmed model-based regulator that stabilizes. By repeatedly improving on a basic model-free controller, they demonstrate significant performance increases and verify the method using a planar Segway simulation. The research [17] examined important safety mechanisms planned and implemented in engineering robotic environments and analyzed to promote safe, collaborative work between people and machines. In addition, the existing regulation has included fresh ideas and a review. The discussion covers multidisciplinary methods such as calculating and evaluating human-robot collision harm, automated software and hardware to reduce human-robot impacts, impact detection technologies, and collision mitigation techniques and minimizing their impact on the suggested strategy for human safety with mobile robots. The hardware configuration for painting is discussed in the article [18], along with current advancements, the lessons learned from previous painting machines, and ideas for novel strategies. They intend to use e-David as a platform for research to enhance automated painting and investigate mechanical creativity. Robotic painting and artificial creativity research exhibit several painting devices, ranging from small, inexpensive plotters to huge industrial robots, and examine the advantages and disadvantages of each type of platform. The article [19] described how DL is used in bone imaging to aid radiologists in finding different anomalies, including fractures. They have also covered the difficulties and issues with the DL-based approach and the potential applications of DL in bone imaging. The study [20] determined a concise assessment of certain AI and ML applications in radiation treatment and discussed relevant factors for improving radiation therapy curricula. The available research shows that typical clinical radiation treatment activities will undergo modifications due to AI and ML techniques. Regulatory barrier components are mathematical compositions to ensure the security of robotic systems. Performance in real-time with instantaneous control synthesis requirements may be accomplished for use with robots by integrating them as restrictions in a quadratic programming optimization trouble.

3. Problem Statement

Consider a robotic system with affine control as in (1) developing in D R 2 and has LiDAR sensors to measure depth. The robot can identify dangerous state space areas using N as the overall sample amount and the depth measuring vector greater than 0 at time t.

Indicate the geometric accuracy of the readings for the LiDAR sensor by θ_{res}. This is the θ_{res} angle formed by two light beams the sensor emits quickly. To take into consideration the physical variations in the workspace's characteristics, we make the following assumption:

Considering that the LiDAR sensor's spatial resolution is adequate to capture a temporal profile of the surrounding area at a certain offset distance, Suppose $r \epsilon V(T; \mathbb{K}^n$m) An insignificant feedback mechanism that the user defines the strategy that the robot will adhere to. Instances of such

Policies might be based on MPC or proportional (go-to-goal) control. Presumably, the state space contains unidentified hazardous areas. This means that for any i 1, 2,..., p, there are p unsafe sets in the state space defined by $V_j = \{y \epsilon T | z_j(y) \leq 0 z_j \epsilon V(T; \mathbb{K})\}$where he is unknown $j \in \{1, 2, \dots, b\}, T | W_{j=1}^{b} V_j$. Ci is the safe area.

Considering the robotic device with quadratic oversight risky sets $V_j \subset T, j \in \{1, 2, \dots, b\}$. Given the theoretical feedback control policy $r : T \rightarrow K$ and LiDAR measures h_d got at every right away $d \geq 0$, formulate an obstacle function production framework which either

1) Learns the hazardous region $W_{j=1}^{b} V_j$ offline provided a dataset of safe and hazardous samples within the domain, or

2) Acquires knowledge the unsafe region via immediate measures h_d as the system travels the domain's boundaries.

4. Methodology

4.1 Generation of regulatory barrier components in robotics using Deep- AntNeuro Colony Net (D-ANCN)

4.1.1 Ant Colony Optimization (ACO)

The ant colony optimization (ACO), initially described by Dorigo and Gambardella, was the first significant enhancement to the original ant optimization to be suggested. The kind of decision rule used by the ants throughout the building process is the first important distinction between ACO and AS. Ants in ACO use the so-called pseudorandom proportional control; the likelihood that an ant will move from city i to city j depends on a random variable q that is uniformly distributed over [0, 1] and a parameterq_0; if $q \leq q0$ the element that maximizes the item's quality ill is selected among the feasible features; otherwise, the same equation as in AS is used.Adding a diversifying element, the local pheromone update balances out this fairly greedy rule, which favors the utilization of the pheromone information. All ants update their local pheromones after each stage of the building. Each and only uses it on the most recent edge they crossed:

$$\tau_{ji} = (1 - \varphi). \tau_{ji} + \varphi. \tau_{ji} \qquad (1)$$

The pheromone's starting value is 0. φ € (0,1] is the pheromone decay coefficient.

The primary objective of the local update is to diversify the future ants' search within one iteration. When edges are traveled, the amount of scent on those edges increases throughout one cycle decreases, encouraging successive ants to choose new boundaries and yield alternate solutions. This reduces the likelihood that many ants will have the same answer during one process. The pheromone's lowest values are also constrained due to the local pheromone update in ACS.

Like AS, ACS also does an offline pheromone update after the building phase.

$$\tau_{ji} \leftarrow (1 - \rho). \tau_{ji} + \rho. \Delta\tau_{ji}^{best} \qquad (2)$$

According to the equation, only edges that were visited by the best and are updated during the ACS offline pheromone update process: where $\Delta\tau_{ji}^{best} = 1/f_{\text{best}}$ otherwise and $\Delta\tau_{ji}^{best} = 0$ depending on whether the best ant utilized side (j,i) on tour. It's important to remember that most of the innovations found in ACS were first introduced in Ant-Q, a predecessor of ACS, by the same authors. Fig 1. Presents the flow of ACO.

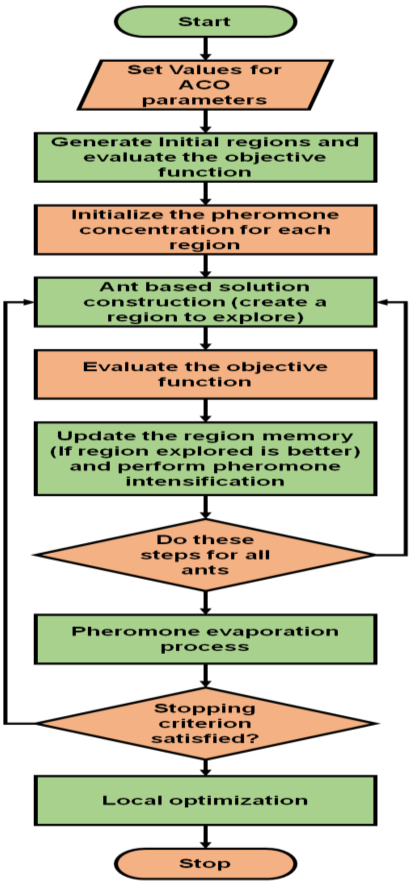

Fig 1. Flow of ant colont optimization (ACO)

3.1.2 Deep Neural Network (DNN)

Three layers: hidden, outputs, and input, make up a DNN model. Fig 2(a) shows the DNN-structure model. The nodes in each layer are hierarchically linked to all other nodes in the coating. The layer after that. Usually, there are just one or two layers in the input and output layers, but there may be two or more levels in the concealed coating. After the output layer is created, prediction values are acquired by processing in the hidden layer using information features provided in the participation coat as input. The prediction strategy of a DNN model is shown in Fig 2(b). All hidden-coat nodes feature a weighted button that accepts the total intake of vertices and turns it into useful principles. The feature mentioned above is used to compute quality estimates and determine the nodes' diagonal sum. The rectified linear unit (ReLU) is the most often used activation function in regression analysis. It provides a value of zero if the weighted sum of the nodes is zero or less than one and a discount equal to the input if it is more than or similar to one.

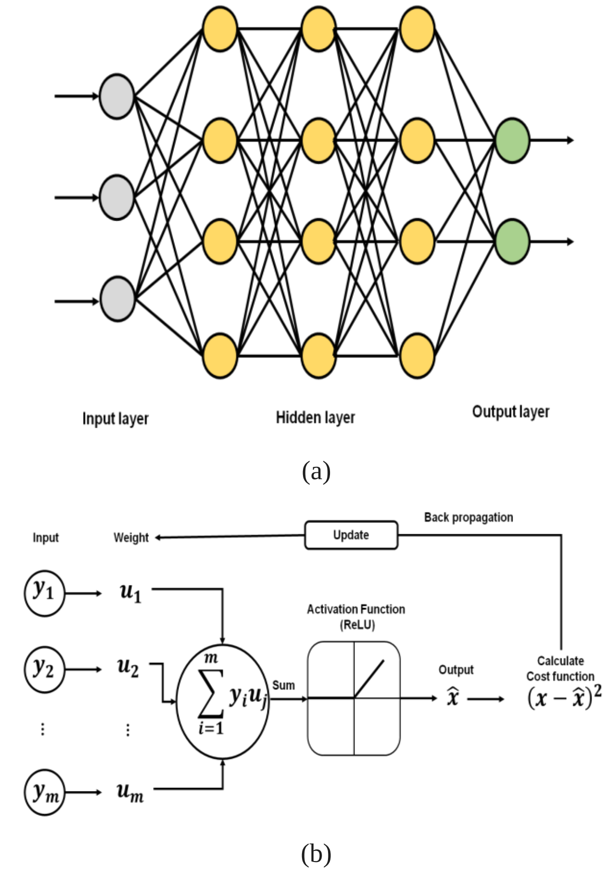

Fig 2. (a) The typical DNN model structure; (b) The basic idea behind utilizing the DNN model to forecast values

During each DNN-model training session, ReLU repeatedly modifies the weight to forecast values. Backpropagation is used to apply this weight alteration of the input coating to the output coating in reverse, awaiting the cost purpose is minimized. The sum of the squares of the discrepancies between the actual and anticipated values may be used to define the cost function. The equation (3) defines the relationship to assess the cost function (E).

$$A = \sum_{r=1}^{m} (x_r - \hat{x}_r)^2 \quad (3)$$

Here, m represents the number of output-layer nodes, and y and y signify the kth output node's observed and forecast values, respectively.

$$u_{ji}^{d} = u_{ji}^{d} - \eta \frac{\partial A}{\partial u_{ji}^{d}} \quad (4)$$

Equation (4) modifies the weight so that the next weight may be taken to equal the difference between the previous weight and the partial derivative of the error function. Here, the letters i, j, and w are the nodes in the preceding and subsequent layers, respectively. It represents the mass at time t and describes the pace of learning.

5. Experimental Results

The "Simple Two Dimensional Robot (STDR) simulator" simulation findings from a route planning viewpoint are described and discussed. For usage in STDR, two environments were developed. Five ellipsoidal obstacles are dispersed across the first environment's 3.3 x 2 workspace region. The more generic impediments in the subsequent set, which has similar size-wise, are difficult to characterize using closed-form polynomial level-sets. In each scenario, the robot follows a notional manager to direct it toward a destination position without previous knowledge of the surroundings.

6. Evaluation Metrics

The rate of association (R) and the Fr'echet distance (F) are two assessment metrics used to compare the trajectory results for the various implementations. These metrics distinguish between the Euclidean distance mismatch and the evolutionary mismatch between trajectories. A way to assess the effects of the suggested algorithms is made possible by combining these two measures.

1. The correlation coefficient informally, the change in one trajectory relative to the other, is captured by the percentage of association for each revolution. In other words, learning how one circuit flows close to another is possible. Two trajectories are often considered to be strongly connected if their correlation coefficients are more than 0.7. When comparing the ground truth data with the trajectory created by the offline and online D-ANCN based techniques, we utilize the connection's strength of form understanding about a course description.

2. Fr'echet Distance: The Fr'echet distance, calculated arbitrarily, compares the Euclidean separations of two paths. The Fr'echet distance expresses the degree of mismatch between two pathways, but the association value indicates how two circuits flow. A smaller Fr'echet distance suggests that the two trajectories are less misaligned. F= 0 specifically means both of the two paths are the same.

7. Results

We start by thinking about the five obstacle scenario. Considered are two alternative robot beginning circumstances. Three distinct paths are displayed. When every obstacle's purpose is understood in advance, the green dashed line shows the ground truth route. This trajectory is produced by solving a QP of the form. The described offline D-ANCN based barrier estimate method had a blue, dotted trajectory. The purple trajectory with dashes is made. This uses the online D-ANCN based technique to estimate the barrier function. Observe how the robots dodge the obstruction and follow in both scenarios. As closely as possible to the nominal control strategy, within the subsequent case, we think about a circumstance where the barrier forms are such that it is difficult to locate the barrier functions' closed-form expressions. The trajectories in green with dashes are produced using the internet D-ANCN Barrier structure-based technique. In contrast, the pink line paths are created using the offline D-ANCN Using the barrier function method explained. An illustration of the calculations' outcomes is also included, shown in Fig 3.

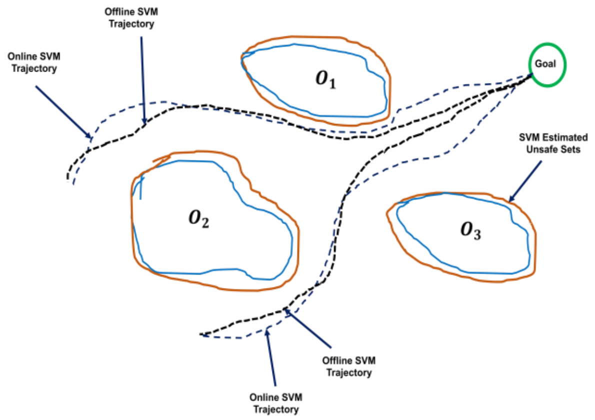

Fig 3. Results of STDR simulator

8. Discussion & Future Scope

Evaluates the relationship coefficients of the offline and online methods to the first scenario's ground truth trajectory. The offline example is also contrasted with the internet approach. A significant degree of resemblance between the barrier and the ground truth trajectory predicted trajectory is shown by the correlation coefficient values we often get, which are > 0.90. The typical relationship between the offline D-ANCN techniques, moreover, the actual velocity is more than 0.97, in particular. The degree of mismatch between two 2D trajectories is then measured using Frechet distances, which are expressed as compared to the distance calculated by Euclid in Fig 4 and Table 1.

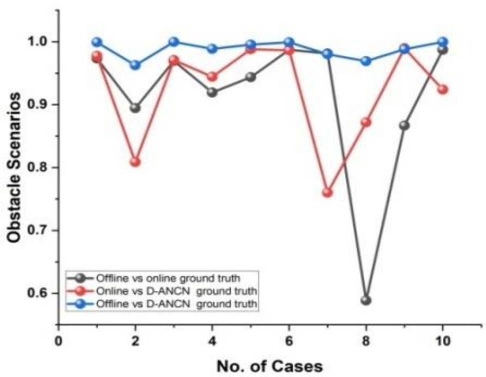

Fig 4. Five Obstacle Scenarios Correlations

Table 1. Coefficients of Correlation for Five Obstacle Scenarios

CASE	OFFLINE VS ONLINE GROUND TRUTH	ONLINE VS D-ANCN GROUND TRUTH	OFFLINE VS D-ANCN GROUND TRUTH
1	0.9735	0.9776	0.9991
2	0.8945	0.8086	0.9626
3	0.9693	0.9708	0.9996
4	0.9194	0.9443	0.9888
5	0.9437	0.9881	0.9955
6	0.9873	0.9864	0.9990
7	0.9812	0.7600	0.9801
8	0.5885	0.8719	0.9691
9	0.8667	0.9898	0.9881
10	0.9873	0.9238	0.9998
average	**0.9113**	**0.9243**	**0.9882**

The mismatch decreases as the Frechet distance decreases between the two paths. The five obstacle scenario's Frechet'distances between trajectories is shown in Fig 5. and Table 2.

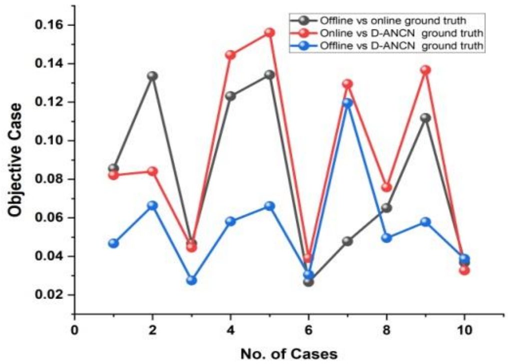

Fig 5. Five-Objective Frechet Range

Table 2. Frechet Range for the Five-Objective Case

Case	Offline vs online ground truth	Online vs d-ancn ground truth	Offline vs d-ancn ground truth
1	0.0855	0.0821	0.0467
2	0.1335	0.0841	0.0663
3	0.0467	0.0445	0.0275
4	0.1231	0.1445	0.0581
5	0.1342	0.1561	0.0661
6	0.0267	0.0391	0.0305
7	0.0478	0.1295	0.1196
8	0.0651	0.0758	0.0495
9	0.1118	0.1367	0.0578
10	0.0368	0.0327	0.0387
average	**0.0812**	**0.0926**	**0.0562**

The fact that we often receive distances of less than 0.10 for each example demonstrates the low magnitude of the disparity in the trajectories' Euclidean distances. The fact that Roofline is quite the magnitude of the Foffline is really small, which indicates that the offline D-ANCN carefully approximated function of barriers resembles the real barrier functions, which is a crucial conclusion from the data above.

Extending the suggested D-ANCN focused education method for synthesizing CBFs to additional antenna types, RGB cameras are an alternative to LIDAR, is one future study path. This might be accomplished by extracting the stereo-depth picture, by it producing a set of practice data, then utilizing it to determine the barrier function.

9. Conclusion

This study described an automated creation of control barrier functions based on computational learning under supervision. The collection of safe and unsafe samples is categorized using a D-ANCN based technique, producing the appropriate barrier (level set) function. Along with formal assurances for the robot's safety, it also guarantees that there will be no misclassification of harmful samples. The suggested framework was assessed by comparing the produced trajectories with actual data. Simulated artificial LiDAR information on an omni robotic in a ROS environment was used in experimental simulations utilizing the proposed framework.

References

[1] Villaronga, E.F., 2019. Robots, standards, and the law: Rivalries between private standards and public policymaking for robot governance. Computer Law & Security Review, 35(2), pp.129-144.

[2] Yang, Y., Zhong, J., Li, W., Gulliver, T.A. and Li, S., 2019. Semisupervised multi-label deep learning-based nonintrusive load monitoring in smart grids. IEEE Transactions on Industrial Informatics, 16(11), pp.6892-6902.

[3] Ada, N., Kazancoglu, Y., Sezer, M.D., Ede-Senturk, C., Ozer, I. and Ram, M., 2021. Analyzing barriers of circular food supply chains and proposing industry 4.0 solutions. Sustainability, 13(12), p.6812.

[4] Wörmann, J., Bogdoll, D., Bührle, E., Chen, H., Chuo, E.F., Cvejoski, K., van Elst, L., Gleißner, T., Gottschall, P., Griesche, S. and Hellert, C., 2022. Knowledge Augmented Machine Learning with Applications in Autonomous Driving: A Survey. arXiv preprint arXiv:2205.04712.

[5] Da, X. and Grizzle, J., 2019. Combining trajectory optimization, supervised machine learning, and

model structure for mitigating the curse of dimensionality in the control of bipedal robots. The International Journal of Robotics Research, 38(9), pp.1063-1097.

[6] Ferraguti, F., Bertuletti, M., Landi, C.T., Bonfè, M., Fantuzzi, C. and Secchi, C., 2020. A control barrier function approach for maximizing performance while fulfilling to iso/ts 15066 regulations. IEEE Robotics and Automation Letters, 5(4), pp.5921-5928.

[7] Flechsig, C., Anslinger, F. and Lasch, R., 2022. Robotic Process Automation in purchasing and supply management: A multiple case study on potentials, barriers, and implementation. Journal of Purchasing and Supply Management, 28(1), p.100718.

[8] Sinha, A., Bagwari, A., Joshi, P., Verma, S. and Kanti, J., 2022. A∗ WRBAS: Space Mobile Robotics Control Conceptual Model Using IoRT Reinforcement Learning and Tracking with Noise Estimation Using EKF. Mobile Information Systems, 2022.

[9] Fountas, S., Espejo-Garcia, B., Kasimati, A., Mylonas, N. and Darra, N., 2020. The future of digital agriculture: technologies and opportunities. IT professional, 22(1), pp.24-28.

[10] Thai, M.T., Phan, P.T., Hoang, T.T., Wong, S., Lovell, N.H. and Do, TN, 2020. Advanced intelligent systems for surgical robotics. Advanced Intelligent Systems, 2(8), p.1900138.

[11] Shorten, C., Khoshgoftaar, T.M. and Furht, B., 2021. Deep Learning applications for COVID-19. Journal of Big Data, 8(1), pp.1-54.

[12] Tripathi, S. and Musiolik, T.H., 2023. Fairness and ethics in artificial intelligence-based medical imaging. In Research Anthology on Improving Medical Imaging Techniques for Analysis and Intervention (pp. 79-90). IGI Global.

[13] Li, X., Tiong, A.M.H., Cao, L., Lai, W., Phan, P.T. and Phee, S.J., 2019. Deep learning for haptic feedback of flexible endoscopic robot without prior knowledge of sheath configuration. International Journal of Mechanical Sciences, 163, p.105129.

[14] Patil, A., Iyer, S. and Pandya, R.J., 2022. A survey of machine learning algorithms for 6g wireless networks. arXiv preprint arXiv:2203.08429.

[15] Mitchell, D., Blanche, J., Harper, S., Lim, T., Gupta, R., Zaki, O., Tang, W., Robu, V., Watson, S. and Flynn, D., 2022. A review: Challenges and opportunities for artificial intelligence and robotics in the offshore wind sector. Energy and AI, p.100146.

[16] Taylor, A.J., Dorobantu, V.D., Le, H.M., Yue, Y. and Ames, A.D., 2019, November. Episodic learning with control Lyapunov functions for uncertain robotic systems. In 2019 IEEE/RSJ International Conference on Intelligent Robots and Systems (IROS) (pp. 6878-6884). IEEE.

[17] Singh Rajawat, A., Bedi, P., Goyal, S.B., Shukla, P.K., Zaguia, A., Jain, A. and Monirujjaman Khan, M., 2021. Reformist framework for improving human security for mobile robots in industry 4.0. Mobile Information Systems, 2021, pp.1-10.

[18] Gülzow, J.M., Paetzold, P. and Deussen, O., 2020. Recent developments regarding painting robots for research in automatic painting, artificial creativity, and machine learning. Applied Sciences, 10(10), p.3396.

[19] Meena, T. and Roy, S., 2022. Bone fracture detection using deep supervised learning from radiological images: A paradigm shift. Diagnostics, 12(10), p.2420.

[20] Chamunyonga, C., Edwards, C., Caldwell, P., Rutledge, P., and Burbery, J., 2020. The impact of artificial intelligence and machine learning in radiation therapy: considerations for future curriculum enhancement. Journal of Medical Imaging and Radiation Sciences, 51(2), pp.214-220.